Taylor & Francis
Taylor & Francis Group

Natural Product Research
Formerly Natural Product Letters

ISSN: 1478-6419 (Print) 1478-6427 (Online) Journal homepage: http://www.tandfonline.com/loi/gnpl20

Solanrubiellin A, a hydroanthraquinone dimer with antibacterial and cytotoxic activity from *Solanum lyratum*

Hui Chen, Kun Du, Yan-Jun Sun, Zhi-You Hao, Yan-Li Zhang, Jiang Bai, Qing-Hua Wang, Hai-Yu Hu & Wei-Sheng Feng

To cite this article: Hui Chen, Kun Du, Yan-Jun Sun, Zhi-You Hao, Yan-Li Zhang, Jiang Bai, Qing-Hua Wang, Hai-Yu Hu & Wei-Sheng Feng (2019): Solanrubiellin A, a hydroanthraquinone dimer with antibacterial and cytotoxic activity from *Solanum lyratum*, Natural Product Research, DOI: 10.1080/14786419.2018.1553173

To link to this article: https://doi.org/10.1080/14786419.2018.1553173

NATURAL PRODUCT RESEARCH
https://doi.org/10.1080/14786419.2018.1553173

Solanrubiellin A, a hydroanthraquinone dimer with antibacterial and cytotoxic activity from *Solanum lyratum*

Hui Chen[a,b], Kun Du[a,b], Yan-Jun Sun[a,b], Zhi-You Hao[a,b], Yan-Li Zhang[a,b], Jiang Bai[c], Qing-Hua Wang[c], Hai-Yu Hu[c] and Wei-Sheng Feng[a,b]

[a]School of Pharmacy, Henan University of Chinese Medicine, Zhengzhou, China; [b]Collaborative Innovation Center for Respiratory Disease Diagnosis, Treatment & Chinese Medicine Development of Henan Province, Henan University of Chinese Medicine, Zhengzhou, China; [c]State Key Laboratory of Bioactive Substance and Function of Natural Medicines, Institute of Materia Medica, Chinese Academy of Medical Scineces and Perking Union Medical College, Beijing, China

ABSTRACT

A new hydroanthraquinone dimer derivative, solanrubiellin A, was isolated from the whole plants of *Solanum lyratum*. The structure of **1** was established through extensive NMR spectroscopy analysis, and the absolute configuration was elucidated by comparison of its experimental and calculated ECD spectra. Compound **1** showed antibacterial activity with MIC values of 2-10 μM against several Gram-positive bacteria. Compound **1** also demonstrated cytotoxic activity against human A549, HT-29 and HL-60 cell lines with IC_{50} values ranging from 2.06 to 9.35 μM.

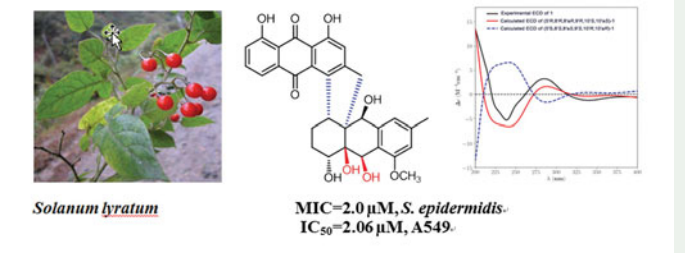

ARTICLE HISTORY
Received 16 October 2018
Accepted 25 November 2018

KEYWORDS
Solanrubiellin A; hydroanthraquinone dimer; *Solanum lyratum*; antibacterial activity; cytotoxic activity

1. Introduction

Solanum is a genus of Solanaceae consisting of more than 1400 species, 40 of which are found in China (Li et al. 2014). *Solanum lyratum* is widely distributed in the southeast of China, partly in Japan, Korea and Indo-China peninsula (Zhang et al. 2012). The whole plants have been used as Chinese traditional medicine (TCM) for more than 2000 years to treat pyretic syndrome and diarrhea, and widely used for the treatment of cancer as a folk remedy (Liu et al. 2011). Previous phytochemistry studies of this

CONTACT Hui Chen chh701@163.com; Yan-Jun Sun sunyanjunily@126.com
Supplemental data for this article can be accessed at https://doi.org/10.1080/14786419.2018.1553173

plant have led to the identification of saponins, steriodal alkaloids, flavonoids, sesquiterpenoids, anthraquinones, courmarins, and fatty acids (Yahara et al. 1985; Ye et al. 2001; Yang et al. 2009). Extensive pharmacological studies indicated that *S.lyratum* possessed antitumor, anti-inflammatory and antibacterial activities (Ling et al. 2013; Wang et al. 2012; Zhang et al. 2010, 2015b). As a part of our continuous effort to search for bioactive constituents from TCM, a new hydroanthraquinone dimer derivative, Solanrubiellin A, was isolated from the CH_2Cl_2 factions of ethanol extract of the whole plant of *S.lyratum*. Herein, we present the isolation, structural elucidation, and antibacterial and cytotoxic activity of **1**.

2. Results and discussion

Compound **1** was obtained as a yellow amporphous powder. Its molecular formula, $C_{31}H_{28}O_9$, was established from NMR data (Table S1) and a prominent pseudomolecular ion peak at *m/z* 567.1637 $[M+Na]^+$ (calcd 567.1626) in HRESIMS, representing 18 degrees of unsaturation. The UV spectrum of **1** showed the maximum absorption bands at 203, 227, 252, 289, and 440 nm, suggesting the presence of the quinone functionality (Huang et al. 2011). The IR spectrum displayed absorptions attributable to hydroxyl (3479 cm^{-1}) and carbonyl (1670 and 1623 cm^{-1}) functions. The ^1H NMR spectrum of **1** was taken in DMSO-d_6 and showed signals for three 1,2,3-trisubstituted aromatic protons at δ_H 7.82 (t, $J=8.5$ Hz, H-6), 7.73 (d, $J=8.5$ Hz, H-5), and 7.36 (d, $J=8.5$ Hz, H-7), an aromatic singlet at δ_H 7.18 (H-2), and two *meta*-substituted aromatic protons at δ_H 6.75 (H-2′) and 6.54 (H-4′). Signals at δ_H 12.50 (s) and 12.0 (s) in the downfield region indicated the presence of two chelating phenolic hydroxyl groups (1-OH and 8-OH). Other signals observed in the ^1H NMR spectrum included four methine protons at δ_H 5.09 (d, $J=4.5$ Hz, H-9′), 4.48 (dd, $J=12.0$, 5.5 Hz, H-5′), 3.95 (brs, H-8′) and 3.50 (d, $J=10.0$ Hz, H-10′), three pairs of methylene protons at δ_H 3.89 (d, $J=17.5$ Hz, H-11a), 2.16 (m, H-7′a), 1.99 (d, $J=17.5$ Hz, H-11b), 1.99 (overlap, H-6′a), 1.58 (m, H-7′b) and 1.42 (m, H-6′b), one methoxy group at δ_H 3.82 (s), and one methyl group at δ_H 2.22 (s). Additionally, four D_2O-exchangeable protons at δ_H 5.19 (10′-OH), 5.02 (8′a-OH), 4.98 (8′-OH), and 4.68 (9′-OH), could also be observed according to the absence of the HSQC correlations. The ^{13}C NMR and DEPT spectra of **1** showed 31 carbon signals, including the characteristic signal due to the quinone carbonyl carbons at δ_C 191.7 (C-9) and 182.5 (C-10), an oxygenated quaternary carbon at δ_C 74.7 (C-8′a), three oxygenated methine carbons at δ_C 73.3 (C-10′), 66.8 (C-8′) and 64.2 (C-9′), three methylene carbons at δ_C 35.7 (C-11), 26.9 (C-7′) and 20.9 (C-6′), one methoxyl carbons at δ_C 55.5, and one methyl carbons at δ_C 21.0 (C-11′). These results suggested that **1** was a dimer of hydroanthraquinone.

To determine the substitution pattern within each of the partial structures of the Abox G ring system of **1**, ^1H-^1H COSY and HMBC experiments were carried out (Figure S1, parts A, B, and C). The connections among the ABC-ring were revealed by the ^1H-^1H COSY correlations from H-5 to H-7 and by the HMBC correlations from 8-OH to C-7, C-8 and C-8a, from H-7 to C-5, C-8 and C-8a, from H-5 to C-7, C-8a and C-10, from 1-OH to C-1, C-2 and C-9a, and from H-2 to C-1, C-4 and C-9a, suggesting the ABC-ring of **1** as a 1,8-dihydroxyanthraquinone moiety (part A). A contiguous

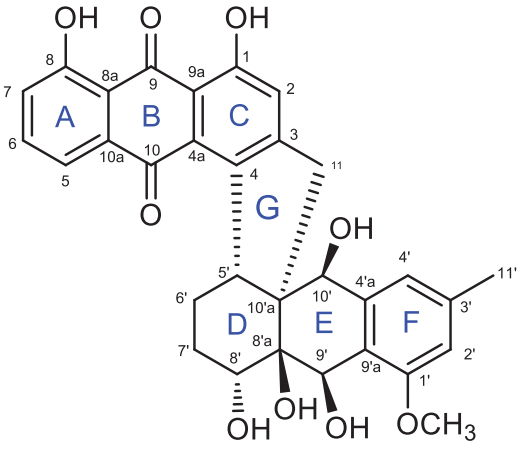

Figure 1. Structure of compound **1**.

sequence of coupled signals from H-5′ to H-8′ in the ^{1}H-^{1}H COSY spectrum combined with the HMBC correlations from H-5′ to C-7′, C-8′a and C-10′ and from H-8′ to C-6′ and C-10′a, established the D-ring of **1** as a cyclohexane moiety. The HMBC correlations from H-9′ to C-1′, C-4′a, C-8′ and C-10′a and from H-10′ to C-4′, C-8′a and C-9′a were observed for connecting the DEF rings (part B). The connection of C-4 (C-ring) and C-5′ (D-ring) was revealed by the HMBC correlations from H-5′ to C-3 and C-4. HMBC correlations from the nonequivalent methylene protons H-11 to C-2, C-3, C-4, C-5′, C-8′a and C-10′ demonstrated that this methylene group linked C-3 and C-10′a, to constitute the G-ring (part C). In addition, the position of the methoxy group was also determined by the HMBC correlation between 1′-OCH_3 and C-1′, and the location of the methyl group was determined by the correction between H-11′ and C-2′ and C-4′. Thus, the planar structure of **1** was determined as shown in Figure 1.

The relative configuration of **1** was determined from NOE correlations in the 1D and 2D ROESY spectrum (Figure S2). The NOE cross peak of H-2 with H_{β}-11 (δ_H 1.99) was much more intense than that of H-2 with H_{α}-11 (δ_H 3.89). The α-position of H-10′ was determined based on the NOE correlations of H-10′ with H-4′ and H_{β}-11. In contrast, the NOE correlations of H-5′ with 10′-OH and H-8′ were observed to establish the β-positions of H-5′ and H-8′. Distinguished from melrubiellin C (Zhang et al. 2015a), compound **1** possessed a unique β-oriented of 8′a-OH and 9′-OH through the diagnostic 1D ROESY correlations of 8′a-OH with H-5′, H-8′, 9′-OH and 10′-OH, and H-9′ with H-8′ and H_{α}-11 (Figure S10). To determined its absolute configuration, a time-dependent density functional theory (TDDFT) method at the B3LYP/6-311G (d, p) level with polarizable continuum model (PCM) in MeOH was performed for (5′*R*,8′*R*,8′a*R*,9′*R*,10′*S*,10′a*S*)-**1** (Figure S13), in which the experimental electronic circular dichroism (ECD) spectrum of **1** was identical to the calculated ECD curve of **1**, indicating that the absolute configuration of **1** was 5′*R*,8′*R*,8′a*R*,9′*R*,10′*S*,10′a*S*. Then, the trivial name solanrubiellin A was proposed for **1**.

Although a variety of dimeric anthraquinones have been reported from natural resources (Socha et al. 2006; Carroll et al. 2012; Xu et al. 2016), the linkage pattern as shown for solanrubiellin A, condensed at C-4box C-5′ and C-11box C-10′a, and the reduction of DE-rings, are quite uncomm. Until now, only four anthraquinone dimer

analogues, melrubiellins A-D, have been reported, but their absolute configurations were not reported (Zhang et al. 2015a, 2015b).

The antibacterial activities of **1** was determined against six terrestrial pathogenic bacteria (*Staphylococcus aureus*, *Staphylococcus epidermidis*, *Enterococcus faecalis*, *Escherichia coli*, *Enterobacter cloacae*, and *Pseudomonas aeruginosa*) (Table S2). Compound **1** exhibited moderate antibacterial activity against *S. aureus* and *E. faecalis* with the MIC values of 2.0 μM (1.08 μg/mL) and 10.0 μM (5.44 μg/mL). Notably, compound **1** showed antibacterial activity against *S. epidermidis* with an MIC value of 2.0 μM (1.08 μg/mL), which was stronger than that of the positive control rifampicin [MIC value, 10.0 μM (8.23 μg/mL)], and same to that of levofloxacin [MIC value, 2.0 μM (0.74 μg/mL)]. Moreover, the cytotoxic activities of **1** was also tested in vitro against five human tumor cell lines (A549, HT-29, HL-60, HepG2, and THP-1) by the MTT assay (Table S3). Compound **1** exhibited cytotoxicity against A549, HT-29, and HepG2 cells, with IC_{50} values ranging from 2.06 to 9.35 μM.

3. Experimental

3.1. General experimental procedures

Optical rotations were obtained on a Rudolph AP-IV polarimeter. UV spectra were measured on a Thermo EVO 300 spectrophotometer. CD spectra were recorded on a JASCO J-815 spectropolarimeter. IR spectra were recorded on a Thermo Nicolet IS 10 spectrometer. NMR spectra were recorded on a Bruker Avance III 500 spectrometer. HRESIMS data were recorded on a Bruker maxis HD Mass Q-TOF LC/MS spectrometer. Preparative HPLC was performed on a Sepuruisi LC-52 instrument with an UV200 detector (Beijing Sepuruisi scientific Co., Ltd., China), using a YMC-pack ODS-A column (250 × 20 mm, 5 μm). Sephadex LH-20 (Amersham Pharmacia Biotech AB, Sweden), ODS (45–70 μm, Merck), and silica gel (200–300 mesh, Qingdao Marine Chemical Inc. China) were used for column chromatography. All solvents were spectroscopic grade or distilled in a glass prior to use.

3.2. Plant materials

The whole plants of *S.lyratum* was collected from Hubei Province, China, in October of 2014, and identified by Prof. Cheng-Ming Dong at Henan University of Chinese Medicine. A voucher specimen (No.20141003B) was deposited in the Department of Natural Medicinal Chemistry, School of Pharmacy, Henan University of Chinese Medicine, Zhengzhou, China.

3.3. Extraction and isolation

Air-dried, powdered whole plants of *S.lyratum* (20 kg) was macerated for 2h with 60 L of 95% EtOH(aq). The residue (1510 g) was suspended in H_2O, followed by successively partition with petroleum ether, CH_2Cl_2, EtOAc, and *n*-BuOH. The CH_2Cl_2 fraction (68 g) was subjected to a silica gel column and eluted with petroleum ether/EtOAc (30:1, 20:1, 10:1, 5:1, 1:1 and 0:1, v/v) to afford seven fractions (A–G). Fraction D (4.7 g) was

subjected to a silica gel column eluting with a step-gradient of petroleum ether/EtOAc (from 5:1 to 2:1) to afford five subfractions C1–C5. Fraction C3 (128 mg) was chromatographed over a sephadex LH-20 column, eluted with MeOH, and further purified by preparative HPLC using the mobile phase MeOH/H_2O (65:35, t_R 42 min) to yield **1** (20.8 mg).

Solanrubiellin A (**1**): yellow amporphous powder; $[\alpha]_D^{25}$ -38.5 (*c* 0.03, $CHCl_3$); UV (MeOH) λ_{max} (log ε) 203 (4.03), 227 (3.91), 252 (3.65), 289 (3.32), 440 (3.35) nm; IR (KBr) ν_{max} 3479, 2925, 1670, 1623, 1459, 1403, 1275, 1212 cm^{-1}; HRESIMS *m/z* 567.1637 $[M+Na]^+$ (calcd for $C_{31}H_{28}O_9Na$, 567.1626). ^1H and ^{13}C NMR data of **1** see Table S1.

3.4. Antibacterial assay

The assay procedure was performed as previously reported (Teng et al. 2016; Zhao et al. 2018; Chu et al. 2018). Levofloxacin and rifampicin were used as the positive control.

3.5. In vitro cytotoxic assay

Compound **1** was evaluated for cytotoxicity against A549 (human lung epithelia cancer), HT-29 (human colon cancer), HL-60 (human promyelocytic leukemia), HepG2 (human hepatocellular carcinoma cancer), and THP-1 (human acute monocytic leukemia) cell lines as per established colorimetric MTT assay protocols (Liu et al. 2018). Adriamycin was used as positive control.

4. Conclusion

In brief, A new hydroanthraquinone dimer derivative, solanrubiellin A, with an uncommon skeleton that condensed at C-4boxC-5′ and C-11boxC-10′a and possessed reduced DE-rings, was isolated from the whole plants of *S. lyratum*. Solanrubiellin A displayed antibacterial activity with MIC values of 2-10 μM against several Gram-positive bacteria. Moreover, it also demonstrated cytotoxic activity against human A549, HT-29 and HL-60 cell lines with IC_{50} values ranging from 2.06 to 9.35 μM. Our study enriched the structure diversity of anthraquinone dimers and the chemistry of *S. lyratum*.

Disclosure statement

No potential conflict of interest was reported by the authors.

Funding

This work was supported by the National Natural Science Foundation of China (No.21602047), the Foundation of Henan Province for Excellent Young Teachers of Colleges and Universities (No. 2017GGJS-081), the Key Projects for Science and Technology Development of Henan (No. 182102310288), and the CAS Innovation Fund for Medical Sciences (CIFMS, No.2017-I2M-4-004).

References

Carroll AR, Nash BD, Duffy S, Avery VM. 2012. Albopunctatone, an antiplasmodial anthrone-anthraquinone from the Australian ascidian *Didemnum albopunctatum*. J Nat Prod. 22: 1206–1209.

Chu WC, Bai PY, Yang ZQ, Cui DY, Hua YG, Yang QQ, Zhang E, Qin S. 2018. Synthesis and antibacterial evaluation of novel cationic chalcone derivatives possessing broad spectrum antibacterial activity. Eur J Med Chem. 143:905–921.

Huang CH, Pan JH, Chen B, Yu M, Huang HB, Zhu X, Lu YJ, She ZG, Lin YC. 2011. Three bianthraquinone derivatives from the mangrove endophytic fungus *Alternaria* sp. ZJ9-6B from the South China Sea. Mar Drugs. 9:832–843.

Li GS, Yao F, Zhang L, Yue XD, Dai SJ. 2014. New sesquiterpenoid derivatives from *Solanum lyratum* and their cytotoxicities. J Asian Nat Prod Res. 16:129–134.

Ling YT, Huang AC, Kuo CL, Yang JS, Lan YH, Yu CC, Huang WW, Chung JG. 2013. Induction of cell cycle arrest and apoptosis in human osteosarcoma U-2 OS cells by *Solanum lyratum* extracts. Nutr Cancer. 65:469–479.

Liu SH, Shen XH, Wei XF, Mao XH. Huang T. 2011. Immunomodulatory activity of butanol extract from *Solanum lyratum* in tumor-bearing mice. Immunopharm. Immunot. 33:100–106.

Liu ZW, Zhang J, Li ST, Liu MQ, Huang XJ, Ao YL, Fan CL, Zhang DM, Zhang QW, Ye WC, Zhang XQ. 2018. Ervadivamines A and B, two unusual trimeric monoterpenoid indole alkaloids from *Ervatamia divaricata*. J Org Chem. 83:10613–10618.

Socha AM, Garcia D, Rowley DC. 2006. Antibiotic bisanthraquinones produced by a Streptomycete isolated from a Cyanobacterium associated with *Ecteinascidia turbinate*. J. Nat. Prod. 69:1070–1073.

Teng P, Huo D, Nimmagadda A, Wu JF, She FY, Su M, Lin XY, Yan JY, Cao AN, Xi CW, et al. 2016. Small antimicrobial agents based on acylated reduced amide scaffold. J Med Chem. 59: 7877–7887.

Wang WC, Hu DY, Yang S. 2012. Study on chemical constituents and bioactivities of plants from *Solanum lyratum* Thunb. Guangzhou Chem. Ind. 39:3–6.

Xu WF, Hou XM, Yang KL, Cao F, Yang RY, Wang CY, Shao CL. 2016. Nigrodiquinone A, a hydroanthaquinone dimer containing a rare C-9–C-7′ linkage from a Zoanthiderived *Nigrospora* sp. fungus. Mar Drugs 2016, 14:51.

Yahara S, Murakami N, Yamasaki, M, Hamada, T, Kinjo JE, Nohara T. 1985. A furostanol glucuronide from *Solanum lyratum*. Phytochemistry. 24:2748–2750.

Yang L, Feng F, Gao Y. 2009. Chemical constituents from *Solanum lyratum*. Chin J Mater Med. 34:1805–1808.

Ye WC, Wang H, Zhao SX, Che CT. 2001. Steroidal glycoside and glycoalkaloid from *Solanum lyratum*. Biochem. Syst. Ecol. 29:421–423.

Zhang CH, Yao DL, Li CS, Luo J, Jin M, Zheng MS, Lin ZH, Jin TF, Li G. 2015a. Cytotoxic anthraquinone dimers from *Melandrium firmum*. Arch Phrm Res. 38:1033–1037.

Zhang CH, Luo J, Li T, Cui Y, Jin M, Yao DL, Zheng M.S, Lin ZH, Cui JM, Li G. 2015b. Chemical constituents from the aerial parts of *Melandrium firmum*. Arch Phrm Res. 38:1746–1751

Zhang DW, Li GH, Yu QY, Dai SJ. 2010. New anti-inflammatory 4-hydroxyisoflavans from *Solanum lyratum*. Chem Pharm Bull. 58:840–842.

Zhang DW, Yang Y, Yao F, Yu QY, Dai SJ. 2012. Solalyratins A and B, new anti-inflammatory metabolites from *Solanum lyratum*. J Nat Med. 66:362–366.

Zhao WW, Zan K, Wu JY, Gao W, Yang J, Ba YY, Wu X, Chen XQ. 2018. Antibacterial triterpenoids from the leaves of *Ilex hainaensis* Merr. Nat. Prod. Res. 1–5.